Polymeric Heterojunction

DOI: 10.1002/anie.201205333

A Facile Band Alignment of Polymeric Carbon Nitride Semiconductors to Construct Isotype Heterojunctions**

*Jinshui Zhang, Mingwen Zhang, Rui-Qing Sun, and Xinchen Wang**

Visible light photocatalysis has attracted great interest, offering a sustainable pathway to drive chemical reactions, such as water splitting and carbon fixation.[1] In principle, heterogeneous photocatalysis involves the generation, migration, and separation of charge carriers in light-excited semiconductors, in which the adsorbed substrates undergo redox reactions with the separated electrons and holes.[2] The photocatalytic performance has been reported to depend on the intrinsic physicochemical properties of semiconductors, including band gap, band position, direct/indirect characters of semiconductor, surface area, particle size, and morphology.[3] During the past 40 years, intensive studies have focused on metal oxides, metal sulfides, and metal nitrides as photocatalysts.[4a,b] Metal-free polymeric semiconductors have recently been introduced as solar-energy transducers and have gained great attentions.[4c] However, the photocatalytic systems developed thus far have been restricted by low efficiency, mainly because of the fast recombination of photoinduced electron–hole pairs.[5]

The band-alignment design of semiconductors is generally adopted to promote the dissociation of excitons and facilitate the subsequent collection and separation of charge at the interfaces of two semiconductors, minimizing charge recombination.[6] There are three classic types of heterojunctions, depending on the band offsets of the two semiconductors, as shown in Scheme 1.[6] Material heterojunctions have, for many years, been applied in semiconductor opto-electronics[6,7] and recently have been extended to photocatalysis for water splitting.[8–10] The creation of tight junctions between two semiconductors not only depends on the electronic structure of the semiconductors but also on other material properties, such as electron affinity and work function.[6] Several kinds of photocatalytic heterojunctions have been developed by coupling different types of photocatalysts. For example, the combination of p-type and n-type semiconductors has been reported to create anisotype p–n photocatalytic diodes, such as p-GaP/n-TiO_2,[8a] p-NiO/n-TiO_2,[8b] and p-$GaFe_2O_4$/n-$PbBi_2Nb_{1.9}W_{0.1}O_9$.[8c] Isotype heterostructural photocatalysts between two different n-type semiconductors have also been developed, mostly based on n-type TiO_2 and coupling to another n-type photocatalysts, for example, CdS/TiO_2,[9a] WO_3/TiO_2,[9b] and ZnO/TiO_2.[9c] Non-TiO_2 based isotype photocatalytic heterojunctions have also been explored, including $BiVO_4$/WO_3,[9d] SnO_2/ZnO,[9e] and ZnO/ZnSe.[9f] The band-structure alignment of these semiconductors creates space charge accumulation/depletion at the interfaces that promotes the separation of photoinduced electrons and holes.[6–9]

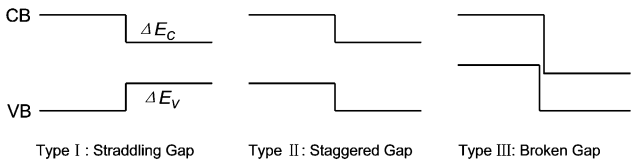

Scheme 1. Three types of semiconductor heterojunctions organized by band alignment. CB: conduction band; VB: valence band. ΔE_C and ΔE_V are the band offsets of CB and VB, respectively.

This strategy was further advanced by constructing isotype heterojunctions between two different crystal phases of a single substance (known as crystal-phase heterojunctions),[10] as in the case of Degussa P_{25} (a mixture of 75% anatase-TiO_2 and 25% rutile-TiO_2).[10a] The slight difference in the electronic band structure between anatase (A) and rutile (R) enables the formation of isotype junction at their crystal interfaces, which well explains the super photocatalytic activity of ultraviolet-excited Degussa P_{25}.[10a,b] Thermal-induced crystal-phase engineering of TiO_2 was reported to form A/R heterojunctions with controlled phase compositions and interfacial domains for long-range charge separation.[10c]

Compared to inorganic semiconductors, which have typical exciton binding energies on the order of 0.01 eV, the fabrication of organic semiconductor heterostructures is especially important because Coulomb binding energies in organic semiconductors are expected, and observed, in the range of several hundred meV for Frenkel exciton, the splitting of which to generate delocalized electron and hole is considered a crucial step towards the application of organic photovoltaic cells.[11] To this end, organic bulk heterojunctions have been developed by solution processing or vacuum sublimation techniques to allow for the absorption of light in the bulk domains to form excitons, followed by charge generation and separation at the interfaces.[7,11] Allowing tuning of their electronic structure by molecular engineering, together with the ease of processing, organic semiconductors are potentially promising for photovoltaic cells and photocatalysis as well. Their use in photocatalysis is however still in

[*] J. Zhang, M. Zhang, Dr. R. Sun, Prof. X. Wang
Research Institute of Photocatalysis, Fujian Provincial Key Laboratory of Photocatalysis-State Key Laboratory Breeding Base, and College of Chemistry and Chemical Engineering, Fuzhou University
Fuzhou 350002 (P. R. China)
E-mail: xcwang@fzu.edu.cn

[**] Supported by the National Basic Research Program of China (973 Program, 2013CB632405) and the National Natural Science Foundation of China (21033003, 21173043, and U1033603).

Supporting information for this article is available on the WWW under http://dx.doi.org/10.1002/anie.201205333.

its infancy as polymers are generally unstable to photocorrosion.[4c]

Recently a binary carbon nitride (CN) based on poly(heptazine) networks as a metal-free photocatalysts for separate water reduction and oxidation has been introduced.[12] This CN photocatalyst is also relevant for the selective conversion of organic compounds, such as alcohol oxidation, oxidative coupling of amines, and oxidative C–C bond formation.[13] In contrary to ordinary conjugated polymers, the CN networks are extremely stable under harsh (photo)chemical and thermal conditions. This is indeed a rare case, but akin to most organic semiconductors, this π-conjugated CN framework is limited by the fast charge recombination.[12] The construction of heterojunctions is therefore desirable as, in principle, it can promote charge separation.

Of particular interest is that the polymeric nature of the semiconductor facilitates the modification of its electronic structure for tuning band offsets. As demonstrated in our earlier work, the molecular engineering of heptazine tectons in a sulfur medium can alter the condensation of CN, greatly adjusting its packing structure and hence tuning the electronic band structure.[14] The CB and VB of sulfur-mediated CN (termed CNS) were determined to be −1.21 and +1.46 V versus Ag/AgCl, approximately 0.2 V more positive than for traditional graphitic CN (CB = −1.42 V, VB = 1.28 V).[12c,14] Such a topology-induced band offset provides an additional opportunity for the easy engineering of isotype heterojunctions based on CN semiconductors, without relying on extra materials.

As illustrated in Scheme 2, once CN and CNS are integrated together, the band alignment between the two materials results in the formation of Type II heterojunction.[6] The CB offset between CN and CNS can drive the migration of photogenerated electrons from CN to CNS, while the photoinduced holes (h^+) are transferred from CNS to CN by the VB offset, both of which help to overcome the high dissociation energy of the Frenkel exciton and help to stabilize electron and hole.[6,11] The redistribution of electrons on one side of the junction (CNS) and holes on the opposite side (CN), greatly reduces the energy-wasteful e^-–h^+ recombination, and thus improving the photocatalytic activity. In addition, with the successful separation of e^-–h^+ pairs, the lifetime of photoinduced charge carriers is efficiently prolonged, which is beneficial for photocatalysis.[10b] The longer lifetime also allows the fast charge transfer across the interfaces to surface-adsorbed substrates on the semiconductor, promoting photoredox reactions. Hence, the creation of heterostructures between CN and CNS is a recommended choice to address the intrinsic drawbacks of CN for photochemical applications.

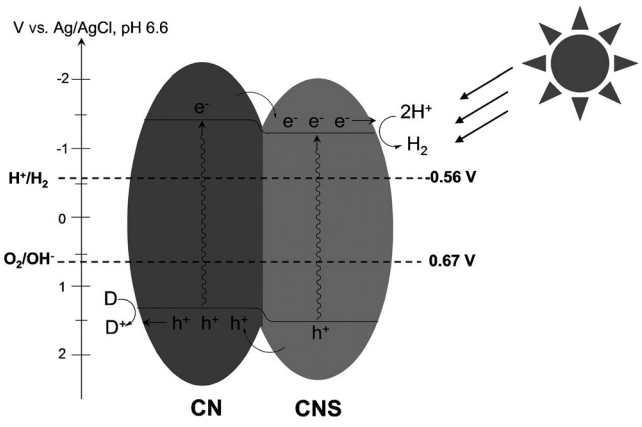

Scheme 2. Schematic illustration of organic heterojunction formed between CN and CNS. D = donor.

It has been demonstrated that there are some docking sites containing -NH_2 groups on the surface of CN polymers, these arise through the defective condensation of CN frameworks.[12] This structure imperfection enables the chemical modification of CN by organic methods. For example, the carbon atom in dicyandiamide (DCDA, the precursor for CN) can electrophilically attack the amino groups on the parent CNS to produce DCDA-grafted CNS hybrids, which can be turned into close-contact CN/CNS junctions after extra thermal sintering to promote the polymerization of DCDA on the surface of CNS.[12d] In principle it should be possible to fabricate, two types of host–guest CN/CNS heterojunctions by the surface-assisted polymerization; CNS–CN (CN serving as the host), and CN–CNS (CNS serving as the host).

To prepare CNS–CN, DCDA was heated at 550 °C for 4 h to produce CN semiconductor. Trithiocyanuric acid (TCA, as the precursor for CNS) was then coated on the surface of CN and then subjected to a heat treatment at 600 °C to induce the formation of CNS on CN. The resultant samples were denoted as CNS-CN-*x*, where *x* (1, 2, 3, 4) refers to the amount of TCA as 10 mg, 30 mg, 50 mg, and 100 mg, respectively. CN–CNS was synthesized by a similar approach, using DCDA and CNS as the CN precursor and the host, respectively. The thus obtained samples were denoted as CN-CNS-*x*, where *x* (1, 2, 3, 4) refers to the amount of DCDA as 30 mg, 100 mg, 200 mg and 500 mg, respectively (see Supporting Information for details).

Note that the physical mixture of CN and CNS failed to produce close interconnection between CN and CNS.

The successful formation of the CNS–CN heterostructure is clearly demonstrated by the TEM images in Figure 1. The big dense thick sheets[12b] and smooth paper-fold thin layers[14] are identified for CN and CNS, respectively (Supporting Information, Figure S1). In the top view (Figure 1a), CNS is found packing closely onto CN, both of which are integrated together as a heterostructure. From the side view (Figure 1b), CNS is grafted on the surface of CN, resulting in the CNS–CN hybrid. These surface-grafted heterostructures were further characterized by the high-resolution X-ray photoelectron spectroscopy (XPS) spectra of S_{2p}. In Figure 1c, two independent binding energy (BE) peaks centering at 159.11 eV and 164.2 eV are found for CNS–CN, but are absent for the host CN. These BE values are close to those of the guest CNS (159.3 eV and 164.2 eV). Thus, the S_{2p} spectra of CNS–CN further confirms the formation of CNS–CN heterostructures. In addition, the BEs of S_{2p} for CNS–CN are quite different from those (163.9 eV and 168.5 eV) on the reported S-doped CN sample,[15] illustrating that the grafted TCA is self-polymerized to CNS, rather than providing a sulfur source

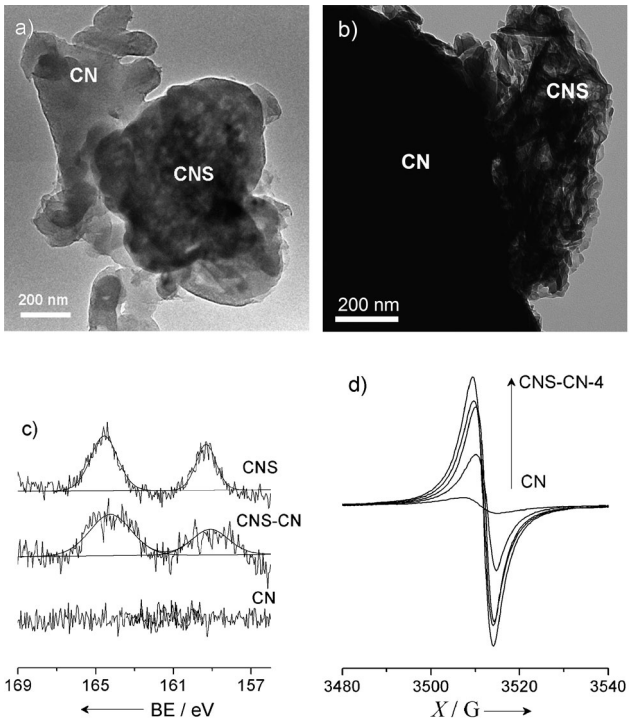

Figure 1. a, b) Typical TEM images of CNS–CN; c) High-resolution XPS spectra of S_{2p} recorded from CN, CNS–CN and CNS; d) Room-temperature EPR spectra of CNS–CN. Arrow direction in (d): CN, CNS–CN-1, CNS–CN-2, CNS–CN-3, CNS–CN-4.

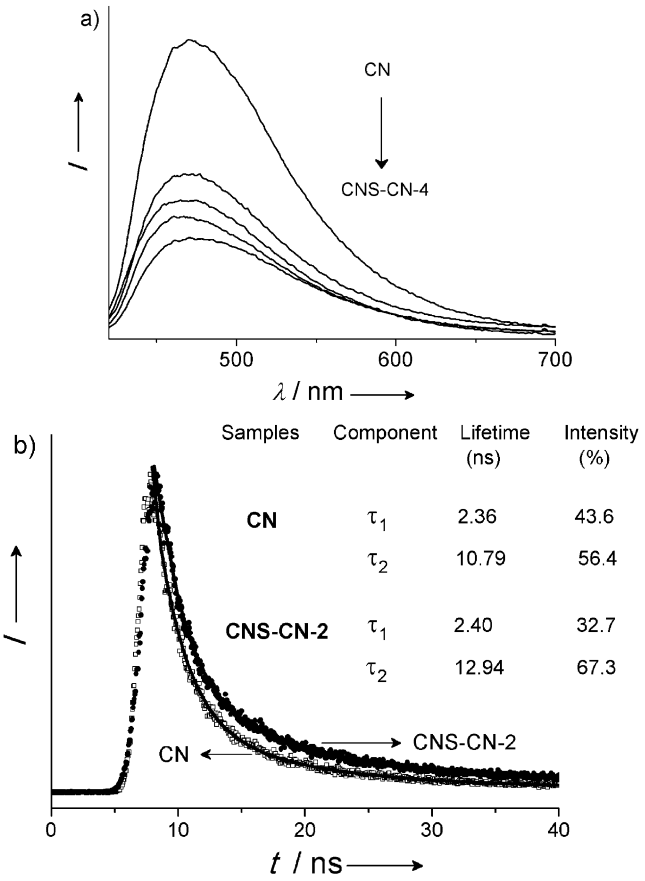

Samples	Component	Lifetime (ns)	Intensity (%)
CN	τ_1	2.36	43.6
	τ_2	10.79	56.4
CNS-CN-2	τ_1	2.40	32.7
	τ_2	12.94	67.3

Figure 2. a) PL spectra recorded at 298 K and b) time-resolved PL spectra monitored at 480 nm under 420 nm excitation at 77 K for CN and CNS–CN.

for doping the CN matrix with sulfur atoms at high temperatures.

The evolution of the electronic band structure for CNS–CN heterojunctions was monitored by electron paramagnetic resonance (EPR) spectra. In Figure 1d, a Lorentzian line centering at $g = 2.0034$ is observed for CN and CNS–CN samples, indicating the generation of unpaired electrons on π-conjugated CN aromatic rings.[12d,f] This Lorentzian line can be greatly enhanced after the formation of heterostructure, presumably due to the redistribution of π electrons within heterojunction by band offsets. Thus, the formation of the heterostructure can help to optimize the electronic band structure for charge migration and separation.

Photoluminescence (PL) emission spectrum originating from the recombination of free charge carriers, usually serves as a good candidate for the characterization of heterostructures, indicating the process of charge migration, transfer and separation.[9,10] In Figure 2a, a strong PL emission peak is observed for the pristine CN, attributed to the radiative recombination of charge carriers. This energy-wasteful process can be greatly suppressed with the localization of electrons in one side (CNS) and holes in the other side (CN) by the band offsets. In addition, the lifetime of charge carriers was also prolonged by the band offsets. For instance, the lifetime of CNS-CN-2 is up to 12.94 ns, about 2.15 ns longer than that of parent CN (10.79 ns; Figure 2b). This prolonged lifetime means the increased probability of electrons or holes that are captured by reactive substrates being available and able to run photoredox functions.

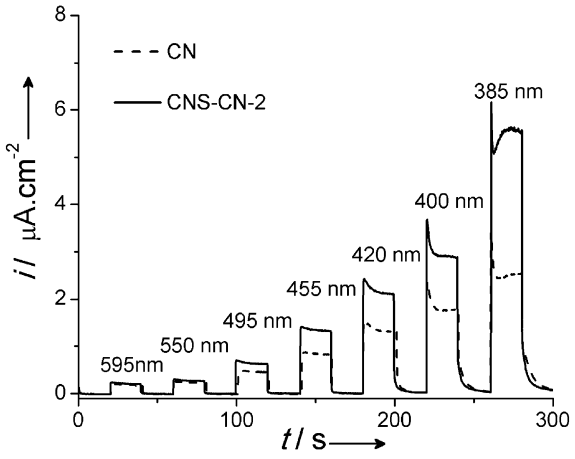

Figure 3. Wavelength dependence photocurrent generation at CN and CNS–CN-2 electrodes in 0.2 M Na_2SO_4 aqueous solution (containing 10 vol.% triethanolamine) without any bias potential.

The photocurrent generation by the heterostructure was examined without any bias potential (Figure 3). Upon light irradiation, a typical n-type photocurrent was produced, indicating the generation and separation of photoinduced e^-–h^+ pairs at CN/water interfaces. As expected, an overall enhanced photocurrent starting from 385 nm to 595 nm is

obtained on CNS–CN-2, attributed to the improved efficiency of charge separation and the prolonged lifetime of charge carriers involved in photoredox reaction. Thus, the intrinsic drawbacks of fast charge recombination in polymeric CN photocatalysts have been addressed by the construction of isotype heterostructures, and a better photocatalytic performance can be expected.

Visible-light-induced H_2 production was investigated to examine the catalytic activity of the samples. As shown in Figure S4, all the CN/CNS heterojunctions demonstrate an enhanced H_2 evolution activity over their corresponding host substrates, and the best samples are CNS–CN-2 and CN–CNS-2, where 11 and 2.3 times higher performance are obtained, respectively. To further underline the necessity of good interconnection for heterojunctions, the physical-mixture samples of CNS + CN and CN + CNS were also tested for photocatalytic activity, and no significant enhancement could be found (Figure S5). Note that the H_2 evolution of CNS–CN heterojunctions can be further improved by creating nanopores in the CN (CNS–MCN, Figure S6), enabling the formation of nanosized CNS–CN heterojunctions which catalyze hydrogen evolution from the protic solution under visible light irradiation.

To further confirm that the high photocatalytic performance was promoted by the generation of isotype heterostructures, rather than the change of physical/chemical characters induced by post-heat treatment. Several physical analyses were performed to characterize the polymeric heterostructure. As shown by X-ray diffraction (XRD) patterns, FT-IR spectra, N_2-sorption analysis and UV/Vis diffuse reflectance spectra (Figures S7–10), the packing motifs, textural structure, and optical absorption properties, which are closely related to the photocatalytic performance, are almost unchanged after the formation of heterojunction. In addition, the post-annealing samples, CN-Heat and CNS-Heat were also examined for photocatalytic H_2 evolution. Only a slightly higher activity was obtained, but this enhancement was by far less than that promoted by the formation of organic heterojunctions (Figure S4).

The durability of heterojunctions acting as photocatalysts for H_2 evolution was evaluated by four consecutive operations. As shown in Figure 4a, the H_2 produced increases steadily with irradiation time, without noticeable deactivation. Additionally, wavelength-dependent H_2 production was also performed on the heterojunction photocatalysts. In Figure 4b, the trend of H_2 production matches well with the optical absorption of the photocatalyst, suggesting that the H_2 evolution reaction (HER) is indeed induced by the excitation of the heterostructure. Meanwhile, an overall enhanced H_2 evolution is observed on CNS–CN-2 across the whole of its absorption spectrum, similar to the photocurrent performance. This wavelength-independent enhancement indicates the band offsets of the heterostructure support visible light photocatalysis.

In conclusion, CN/CNS isotype heterojunctions were prepared in an approach based on by the band alignment between CN and CNS, thus exploiting the slight difference in their electronic band structures. Such a polymeric isotype heterojunction was demonstrated to promote charge separation which arises from the band offsets, leading to a significant enhancement in the photocatalytic activity for hydrogen evolution. The heterostructure strategy demonstrated herein offers new opportunities for sustainable utilization of solar irradiation by using readily prepared polymers as energy transducers and constructing an isotype/anisotype dyadic layering on the various nanostructured and copolymerized CN frameworks[12,16] to promote exciton dissociation and charge separation. These CN nanoheterojunctions can also be envisaged to be useful in other areas, such as organic photosynthesis and photovoltaic devices.

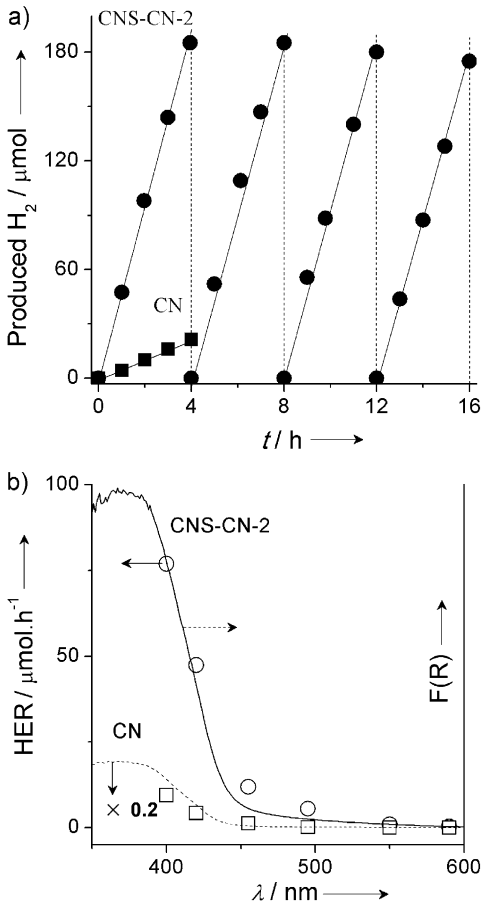

Figure 4. a) Stability test of H_2 evolution (evacuation every 4 h) for CNS–CN-2 photocatalyst under visible-light irradiation ($\lambda > 420$ nm), together with pristine CN as the reference. b) Wavelength dependence of H_2 evolution from water by CN (squares) and CNS–CN-2 (circles). The optical absorption spectrum of CN was multiplied by 0.2.

Received: July 6, 2012
Published online: September 7, 2012

Keywords: band alignment · carbon nitride · heterojunctions · photocatalysis · semiconductors

[1] See for example: a) N. Lewis, D. Nocera, *Proc. Natl. Acad. Sci. USA* **2006**, *103*, 15729; b) X. Chen, S. Shen, L. Guo, S. Mao, *Chem. Rev.* **2010**, *110*, 6503; c) S. In, D. Vaughn II, R. Schaak,

Angew. Chem. **2012**, *124*, 3981; *Angew. Chem. Int. Ed.* **2012**, *51*, 3915.

[2] K. Maeda, A. Xiong, T. Yoshinaga, T. Ikeda, N. Sakamoto, T. Hisatomi, M. Takashima, D. Lu, M. Kanehara, T. Setoyama, T. Teranishi, K. Domen, *Angew. Chem.* **2010**, *122*, 4190; *Angew. Chem. Int. Ed.* **2010**, *49*, 4096.

[3] See for example: a) A. Linsebigler, G. Lu, J. Yates, *Chem. Rev.* **1995**, *95*, 735; b) A. Hagfeldt, M. Grätzel, *Chem. Rev.* **1995**, *95*, 49.

[4] See for example: a) F. Osterloh, *Chem. Mater.* **2008**, *20*, 35; b) K. Maeda, K. Domen, *Chem. Mater.* **2010**, *22*, 612; c) M. Schwab, M. Hamburger, X. Feng, J. Shu, H. Spiess, X. Wang, M. Antonietti, K. Müllen, *Chem. Commun.* **2010**, *46*, 8932.

[5] K. Maeda, K. Domen, *J. Phys. Chem. Lett.* **2010**, *1*, 2655.

[6] See for example: a) Z. Alferov, *Semiconductors* **1998**, *32*, 1; b) J. Tersoff, *Phys. Rev. B* **1984**, *30*, 4874.

[7] See for examples: a) J. Peet, A. Heeger, G. Bazan, *Acc. Chem. Res.* **2009**, *42*, 1700; b) R. Giridharagopal, D. Ginger, *J. Phys. Chem. Lett.* **2010**, *1*, 1160.

[8] a) A. Nozik, *Appl. Phys. Lett.* **1976**, *29*, 150; b) J. Yu, W. Wang, B. Cheng, *Chem. Asian J.* **2010**, *5*, 2499; c) H. Kim, P. Borse, W. Choi, J. Lee, *Angew. Chem.* **2005**, *117*, 4661; *Angew. Chem. Int. Ed.* **2005**, *44*, 4585.

[9] a) X. Gao, W. Sun, Z. Hu, G. Ai, Y. Zhang, S. Feng, F. Li, L. Peng, *J. Phys. Chem. C* **2009**, *113*, 20481; b) S. Chai, Y. Kim, W. Lee, *J. Electroceram.* **2006**, *17*, 909; c) D. Kim, S. Lee, H. Jung, J. Kim, H. Shin, K. Hong, *Int. J. Hydrogen Energy* **2007**, *32*, 3137; d) S. Hong, S. Lee, J. Jang, J. Lee, *Energy Environ. Sci.* **2011**, *4*, 1781; e) L. Zheng, Y. Zheng, C. Chen, Y. Zhan, X. Lin, Q. Zheng, K. Wei, J. Zhu, *Inorg. Chem.* **2009**, *48*, 1819; f) P. Chen, L. Gu, X. Cao, *CrystEngComm* **2010**, *12*, 3950.

[10] a) T. Kawahara, Y. Konishi, H. Tada, N. Tohge, J. Nishii, S. Ito, *Angew. Chem.* **2002**, *114*, 2935; *Angew. Chem. Int. Ed.* **2002**, *41*, 2811; b) V. Etacheri, M. Seery, S. Hinder, S. Pillai, *Chem. Mater.* **2010**, *22*, 3843; c) J. Zhang, Q. Xu, Z. Feng, M. Li, C. Li, *Angew. Chem.* **2008**, *120*, 1790; *Angew. Chem. Int. Ed.* **2008**, *47*, 1766.

[11] a) C. Piliego, M. Loi, *J. Mater. Chem.* **2012**, *22*, 4141; b) M. Muntwiler, Q. Yang, X. Zhu, *J. Electron Spectrosc. Relat. Phenom.* **2009**, *174*, 116.

[12] a) X. Wang, K. Maeda, A. Thomas, K. Takanabe, G. Xin, J. Carlsson, K. Domen, M. Antonietti, *Nat. Mater.* **2009**, *8*, 76; b) X. Wang, K. Maeda, X. Chen, K. Takanabe, K. Domen, Y. Hou, X. Fu, M. Antonietti, *J. Am. Chem. Soc.* **2009**, *131*, 1680; c) J. Zhang, X. Chen, K. Takanabe, K. Maeda, K. Domen, J. Epping, X. Fu, M. Antonietti, X. Wang, *Angew. Chem.* **2010**, *122*, 451; *Angew. Chem. Int. Ed.* **2010**, *49*, 441; d) J. Zhang, G. Zhang, X. Chen, S. Lin, L. Möhlmann, G. Dołęga, G. Lipner, M. Antonietti, S. Blechert, X. Wang, *Angew. Chem.* **2012**, *124*, 3237; *Angew. Chem. Int. Ed.* **2012**, *51*, 3183; e) J. Zhang, M. Grzelczak, Y. Hou, K. Maeda, K. Domen, X. Fu, M. Antonietti, X. Wang, *Chem. Sci.* **2012**, *3*, 443; f) J. Zhang, M. Zhang, G. Zhang, X. Wang, *ACS Catal.* **2012**, *2*, 940.

[13] a) X. Wang, S. Blechert, M. Antonietti, *ACS Catal.* **2012**, *2*, 1596; b) F. Su, S. Mathew, L. Mohlmann, M. Antonietti, X. Wang, S. Blechert, *Angew. Chem.* **2011**, *123*, 683; *Angew. Chem. Int. Ed.* **2011**, *50*, 657.

[14] J. Zhang, J. Sun, K. Maeda, K. Domen, P. Liu, M. Antonietti, X. Fu, X. Wang, *Energy Environ. Sci.* **2011**, *4*, 675.

[15] G. Liu, P. Niu, C. Sun, S. Smith, Z. Chen, G. (Max) Lu, H. Cheng, *J. Am. Chem. Soc.* **2010**, *132*, 11642.

[16] a) X. Li, J. Zhang, X. Chen, A. Fischer, A. Thomas, M. Antonietti, X. Wang, *Chem. Mater.* **2011**, *23*, 4344; b) X. Chen, Y. Jun, K. Takanabe, K. Maeda, K. Domen, X. Fu, M. Antonietti, X. Wang, *Chem. Mater.* **2009**, *21*, 4093; c) E. Lee, Y. Jun, W. Hong, A. Thomas, M. Jin, *Angew. Chem.* **2010**, *122*, 9900; *Angew. Chem. Int. Ed.* **2010**, *49*, 9706.

